Journal of Southeast University (English Edition) Vol. 31, No. 1, pp. 100 - 106 Mar. 2015 ISSN 1003—7985

Variable damping forces caused by electromagnetic energy harvesting with an adjustable load

Li Chuan[1] Zhu Rongrong[1] Feng Xin[1] Yang Shuai[2]

([1]Chongqing Joint International Research Center of System Health Maintenance, Chongqing Technology and Business University, Chongqing 400067, China)

([2]Department of Mechanical Engineering, University of Ottawa, Ottawa K1N 6N5, Canada)

Abstract: A novel variable damper using an adjustable energy harvesting structure is proposed for semi-active vibration systems. The fluid flowing in a hydraulic cylinder is employed to drive an electromagnetic generator for harvesting vibration energy, which on the other hand, leads to a damping effect of the hydraulic damper. To make the damping force variable, an adjustable resistor is adopted to tune the capability of energy harvesting. The present approach is validated by both theoretical analysis and experimental evaluation. When connected with different resistance loads, the prototype damper has different equivalent damping coefficients ranging from 3.987×10^4 to 2.488×10^5 N · s/m. The results show that the damping force of the damper is variable in response to the adjustable load for the vibration energy harvesting.

Key words: variable damper; vibration; energy harvesting; electromagnetic generator; load

doi: 10.3969/j.issn.1003 - 7985.2015.01.017

Dampers have been widely used in automobiles, motorcycles, wheeled or tracked vehicles, aircrafts, as well as some industrial machines[1]. Dry friction, fluid friction, hysteresis of structural material, and magnetic effects have been used to generate a damping force for the dampers[2-3]. However, the dampers are often energy-wasting components[4]. The energy consumed by the dampers has a great potential for real applications if harvested[5]. For a passenger car traversing on poor road surface at around 48 km/h (13.4 m/s), for example, the wasted energy of four dampers is approximately 200 W[6]. Moreover, the dissipated energy may generate noise and heat that are harmful to the vehicle and the environment. Therefore, energy harvesting from the damping component is a win-win strategy.

Different approaches have been developed for integrating the energy harvester with the damper. Chen and Liao[7] introduced a self-sensing magnetorheological damper that integrated energy harvesting, dynamic sensing and damping into one device. Choi et al.[8] suggested integrating an electromagnetic-induction device into a magnetorheological damper for harvesting energy from shocks and vibrations. A linear multi-pole electromagnetic generator was used to collect the energy at around 0.1 W. Sapiński[9] introduced an electromagnetic power generator for a linear magnetorheological damper. Suda et al.[10] developed a hybrid suspension system by employing a linear DC generator to harvest vibration energy for active vibration control. Choi and Wereley[11] proposed a self-powered magnetorheological damper integrating a spring-mass with an electromagnetic induction device. Choi et al.[12] applied a rack-pinion mechanism to amplify the vibration response for providing more power to control an electrorheological damper. Aly et al.[13] used a lever mechanism incorporating a smart damper to improve the flexural response of a very slender building. Fang et al.[14] developed a hydraulic electromagnetic shock absorber using separated components. The energy recovery efficiency is only 16.6% in 10 Hz sinusoidal excitation with a 3 mm amplitude. Li et al.[15] applied an inverse screw transmission for a two-terminal flywheel to convert the oscillatory vibration into the reciprocating rotation of the flywheel. By adjusting the transmission ratio between the rectilinear vibration and the bidirectional rotation, an electro-hydraulic approach was developed to realize a variable inertial mass[16].

By adjusting the damping effect, on the other hand, variable dampers have been developed as key components for semi-active vibration systems. Hence, in this work, we employ an adjustable energy harvesting structure to introduce a variable damping force for the damper.

Hydraulic dampers are capable of yielding a greater damping force mainly by means of fluid friction, and are able to work under harsh impulses. For these reasons, the hydraulic dampers enjoy one of the largest shares in the current damper market. In this research, the fluid flowing in a hydraulic damper is employed to drive an electromagnetic generator for harvesting the vibration energy, which on the other hand leads to a damping effect

Received 2014-07-01.

Biography: Li Chuan (1975—), male, doctor, professor, chuanli@21cn.com.

Foundation items: The National Natural Science Foundation of China (No. 51375517), the Natural Science Foundation of CQ CSTC (No. 2012JJJQ70001), the Project of Chongqing Innovation Team in University (No. KJTD201313).

Citation: Li Chuan, Zhu Rongrong, Feng Xin, et al. Variable damping forces caused by electromagnetic energy harvesting with an adjustable load[J]. Journal of Southeast University (English Edition), 2015, 31(1): 100 - 106. [doi: 10.3969/j.issn.1003 - 7985.2015.01.017]

on the hydraulic damper. To make the damping force variable, an adjustable load is suggested for tuning the capability of the energy harvesting. The present approach is validated by both theoretical analysis and experimental evaluation.

1 Methodology

1.1 Schematic illustration

Usually, the dampers dissipate the vibration energy as thermal energy, acoustic energy and/or other types of energy. In view of the energy conservation, the vibration energy harvesters are also special dampers which transform the vibration energy into electricity. Based on this observation, we propose a novel damper as illustrated in Fig. 1 to validate our idea for a variable damping force resulting from adjustable vibration energy harvesting.

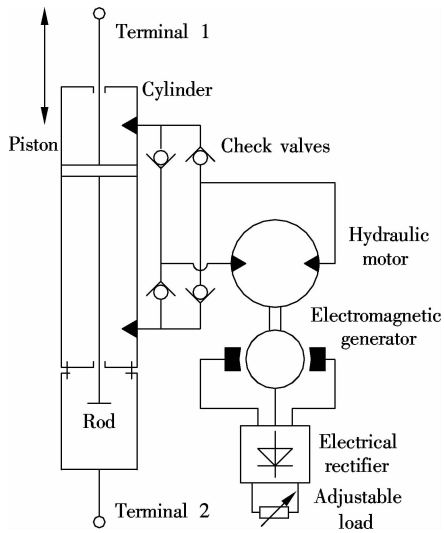

Fig. 1 Schematic diagram of the proposed variable damper

As shown in Fig. 1, an electromagnetic energy-harvesting structure is proposed as an auxiliary part of a hydraulic cylinder. Similar to conventional hydraulic dampers, the core of our structure is the hydraulic cylinder, which is divided into two chambers by a piston. Two rods, across the two chambers, connect with two sides of the piston, respectively. The reason for using the two-rod cylinder is to guarantee identical oil flowing between the two chambers. One of the rods is attached directly to one terminal of the damper, while another one is sheltered by a cap, to which another terminal is connected. As shown in Fig. 1, the two ports of the cylinder are connected to the two ports of a hydraulic motor via four check valves. The output shaft of the hydraulic motor is connected to an electromagnetic generator, whose output electricity is used to power a load resistor through an electrical rectifier. The proposed structure makes it possible for the rectilinear vibration between the two terminals of the damper to be used to drive the unidirectional rotation of the hydraulic motor in a smooth manner, and generate electricity from the load at the same time. The vibration energy is absorbed as a result of 1) Energy harvesting by the load, and 2) Energy dissipation through the oil flowing and the motion transmission. Apparently, the damping force can be achieved using the proposed design.

As shown in Fig. 1, there are four check valves composing a bridge configuration. In response to either the positive vibration or the negative vibratory excitation (i.e., compression between the two terminals), the rotation of the hydraulic motor (and the power generator) is always unidirectional, though the vibratory excitation is bidirectional. To make energy harvesting variable, an adjustable resistor is employed as the load of the damper. In this research, the resistor is tuned manually. As for industrial applications, the resistor can be easily adjusted by electric circuits. Therefore, the present approach delivers an electric means towards the variable damping design.

1.2 Theoretical analysis

To validate our approach in generating variable damping force using adjustable energy harvesting, we perform a theoretical analysis on the conceptual design as shown in Fig. 1.

With a vibratory excitation $x(t)$ where t is the time, the mechanical behavior of the proposed damper can be approximated by Fig. 2.

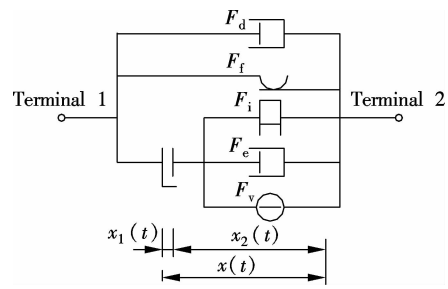

Fig. 2 Mechanical model of the proposed damper

As shown in Fig. 2, the vibratory excitation $x(t)$ can be divided into two constituents: the backlash $x_1(t)$ caused by the hydraulic transmission, and the effective excitation $x_2(t)$ to drive the generator. Upon neglecting the elasticity of the system, there are five different forces related to $x_1(t)$ and/or $x_2(t)$, respectively. According to the mechanical model as shown in Fig. 2, the five forces are introduced in detail as follows:

1) Oil damping force $F_d(t)$. The flow of the oil inside the absorber results in a viscous damping effect, which is given by

$$F_d(t) = c_s \dot{x}(t) \tag{1}$$

where c_s denotes the equivalent viscous damping coefficient of the hydraulic system.

2) Friction force $F_f(t)$. Supposing that the value of the piston friction is f_0, the friction force is formulated as

$$F_f(t) = -\operatorname{sgn}(\dot{x}(t))\,|f_0| \tag{2}$$

where $\dot{x}(t)$ is the first derivative of $x(t)$ with respect to t, and $\operatorname{sgn}(\cdot)$ is the sign function.

3) Inertial force $F_i(t)$. The inertial force is mainly caused by the rotation of the rotor of the generator. Letting m denote the equivalent inertial mass of the rotor, the inertial force is given by

$$F_i(t) = m\ddot{x}_2(t) \tag{3}$$

It should be noted that the equivalent inertial mass m is neither the gravitational mass nor the moment of inertia of the rotor. Instead, the equivalent inertial mass is associated with both the transmission ratio and the moment of inertia of the rotor. For more details on the calculation of the equivalent inertial mass m, one can refer to our former work[17].

4) Energy-harvesting induced force $F_e(t)$. According to the law of conservation of energy, the harvested energy by the load resistor R_d is equal to the input power of the generator, i.e.,

$$F_e(t)\dot{x}_2(t) = (i(t))^2 R_d \tag{4}$$

For a three-phase electromagnetic generator, one has

$$i(t) = \sqrt{3}\,\mathrm{mod}\left(\frac{k_m\omega}{\mathrm{j}L_1\omega + R_1 + R_d}\right) \tag{5}$$

where k_m stands for the electromotive voltage constant; ω represents the angular velocity; L_1 represents the internal inductance; and R_1 denotes the internal resistance of one phase. Suppose that

$$\omega(t) = k_\omega \dot{x}(t) \tag{6}$$

where k_ω is the ratio of $\dot{x}(t)$ to $\omega(t)$. One can obtain the following equation from Eqs. (4) to (6):

$$F_e(t) = c_e\dot{x}_2(t) \tag{7}$$

where

$$c_e = 3\,\mathrm{mod}\left(\frac{k_m k_\omega}{\mathrm{j}L_1\omega + R_1 + R_d}\right)^2 R_d \tag{8}$$

5) Opening force $F_v(t)$ of the check valves. Denoting the opening pressure of a check valve by P_c, one has

$$\left.\begin{aligned} F_v(t) &= 2P_cS_c \qquad x_1(t) = 0 \\ F_v(t) &= 0 \qquad\quad |x_1(t)| > 0 \end{aligned}\right\} \tag{9}$$

where S_c is the cross-sectional area of the cylinder.

One may notice that there are two conditions for the mechanical model as shown in Fig. 2: contact and backlash conditions. If the maximum backlash is δ and the bidirectional backlashes are identical, one has

$$\delta \geqslant |x_1(t)| \geqslant 0 \tag{10}$$

Having analyzed the five force components and the contact/backlash conditions, the mechanical governing equation of the absorber in response to the shock excitation $x(t)$ can be therefore obtained as

$$\left.\begin{aligned} F(t) &= F_d(t) + F_f(t) + F_i(t) + F_e(t) + F_v(t) \\ &\qquad\qquad x_1(t) = 0 \\ F(t) &= F_d(t) + F_f(t) \qquad |x_1(t)| > 0 \end{aligned}\right\} \tag{11}$$

The proposed design can be regarded as a system with one input $x(t)$ and two output variables $F(t)$ and $v(t)$ (or $i(t)$ and $P_d(t)$). Based on the above mechanical governing equation and letting $y_1(t) = F(t) - F_f(t)$, the mechanical transfer function under the backlash condition is given by

$$\mathrm{TF}_1(s) \approx c_s s \leftrightarrow \frac{y_1(t)}{x(t)} \tag{12}$$

where s is Laplace's complex variable; $\mathrm{TF}_1(s)$ is the mechanical transfer function under the backlash condition. Under the contact condition, moreover, letting $y_2(t) = F(t) - F_f(t) - F_v(t)$ and omitting the effect of the backlash, the mechanical transfer function $\mathrm{TF}_2(s)$ can be expressed as

$$\mathrm{TF}_2(s) \approx ms^2 + c_s s + c_e s \leftrightarrow \frac{y_2(t)}{x(t)} \tag{13}$$

On the other hand, the transfer function between $x(t)$ and $v(t)$ is valid only under the contact condition. The electrical transfer function can be deduced from Eq. (13) as

$$\mathrm{TF}_3(s) \approx \sqrt{3}\,\mathrm{mod}\left(\frac{k_m k_\omega}{L_1 s + R_1 + R_d}\right) s \leftrightarrow \frac{v(t)}{x(t)} \tag{14}$$

It is worth noting that the electromechanical model as illustrated by Eqs. (12) to (14) is a simplified expression as most of nonlinear parameters are omitted or linearized. Nevertheless, the above electromechanical model can provide an intuitive understanding of the proposed damper. Hence, we apply the above electromechanical model to analyze how the variable damping force can be achieved by tuning load resistance.

As shown in Eq. (13), c_s is merely the electricity-induced damping coefficient. The variable damping force can be achieved by adjusting c_s. According to Eq. (8), five parameters, i.e., k_m, k_ω, L_1, R_1, and R_d, are available for adjusting c_s. For a given structure as shown in Fig. 1, unfortunately, only R_d can be easily tuned in reality. Hence, one can tune the load resistance R_d to adjust c_s, and further the damping force of the damper. Therefore, the theoretical analysis reveals that the damping forces can be made variable through adjusting the load resistance for electromagnetic energy harvesting as shown in Fig. 1.

2 Experiments

2.1 Prototyping

In addition to the theoretical analysis, we also carried out experiments to prove that the damping force can be made variable though adjustable vibration energy harvesting for the hydraulic damper.

Based on the schematic illustration as shown in Fig. 1, a prototype device was fabricated at Chongqing Technology and Business University. A steel frame with the rod cap was fabricated to accommodate all the parts shown in Fig. 1. The oil cylinder with an internal diameter of 40 mm and a maximum travel of 80 mm was installed on the steel frame. The hydraulic rectifier and the hydraulic motor were fixed on the two sides of the cylinder. Four check valves, each of which has a nominal diameter of 10 mm and an opening pressure of 0.2 MPa, were used for the prototype device. The displacement of the hydraulic motor (BMM8-MAE) was 8.2 mL per revolution. The permanent-magnet generator was connected to the output shaft of the hydraulic motor via a coupling. The nominal rotational speed of the generator was 500 r/min. The output of the power generator was connected to the electrical rectifier (30 A, 600 V), which was used to power the load resistor directly.

To assemble the hydraulic circuit, four custom-made brass tubes (8 mm in diameter) were used to integrate the aforementioned parts together. For oil filling, exhausting and refilling as necessary, a 8 mm nominal diameter release valve was also connected to one of the brass tubes. The electric parameters of the harvester were measured as: $R_1 = 7.6\ \Omega$, $L_1 = 0.02$ H and $k_m = 0.57$ V·s/rad.

2.2 Experimental setup

As shown in Fig. 3, the prototype device of the damper was fixed on an electro-hydraulic servo fatigue test machine (20 kN), which was controlled by a desktop computer via a controller. The testing machine was driven by a hydraulic source (30 L/min). According to the vibration signal $x(t)$ predefined by the computer, the lower terminal of the specimen moves up and down, yielding a unidirectional rotation ($\omega(t)$) of the hydraulic motor and a relative force ($F(t)$) between the two terminals of the specimen. The actual vibration displacement and the mechanical force were acquired by the computer via the controller. An adjustable resistor (0-50 Ω) was used as the load that was measured by a multi-meter. The generated voltage ($v(t)$) of the load was measured by an oscillator, and then fed to the computer for recording.

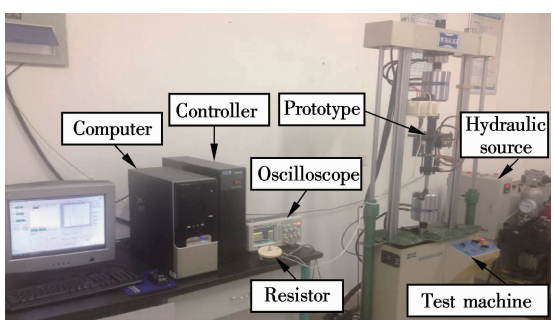

Fig. 3 Experimental setup

3 Results and Discussion

Setting the vibration signal $x(t)$ to be $0.01\sin\pi t$ (m) and $0.015\sin\pi t$ (m), we tune the resistor at 2.5, 5, 7.5, 10, 15, 50, and $+\infty\ \Omega$ (open circuit). For 50 Ω and $+\infty\ \Omega$ experiments, the vibratory amplitude was set as 0.015 m to reduce the influence of the backlash. As for the rest of the resistances, the amplitude was chosen as 0.01 m (in these cases, 0.015 m amplitude may cause too great forces to be endured by the test machine). Fig. 4 plots the change of the vibration force in response to the change in the vibratory displacement. It was observed that the damping loop was not saturated. In other words, evident spikes occurred at 50 Ω and $+\infty\ \Omega$ experiments. This is mainly due to the existence of the backlash. As for the 2.5-15 Ω cases, the spikes are released by the improved energy-harvesting which is an equivalent of the increased damping force. The same phenomenon has always been observed by Papageorgiou et al[18]. When testing inerter devices using a similar testing machine, they observed evident spikes which were worse than those in our cases. They developed a "buffer network" to introduce the damping force to suppress the spikes. Fortunately, our device is capable of buffering itself due to the electricity-induced damping force.

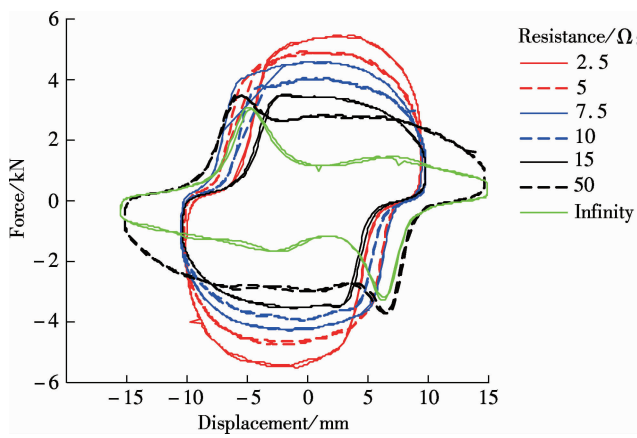

Fig. 4 Vibration forces in response to vibratory displacements with different resistances

For the vibration applications, the input power $P_{in}(t)$ resulting from the vibratory excitation can be obtained by

$$P_{in}(t) = F(t)\dot{x}(t) \tag{15}$$

Under different resistance loads, the input powers of

the vibratory excitations can be calculated, which are shown in Fig. 5.

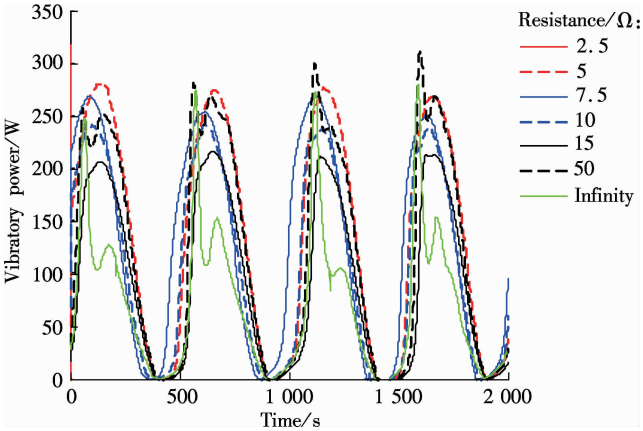

Fig. 5 Vibratory powers of the seven experiments

Under different vibratory excitations and loads, the damper is capable of harvesting power. Fig. 6 displays the harvested power by the damper. It is noted that, under open circuit ($+\infty\ \Omega$), none of the power can be harvested. Therefore, there are merely six output curves for the harvested electricity.

Fig. 6 shows that the peak value for 50 Ω load is apparently staggered with other peak values. This is caused by the spike effects as shown in Fig. 4 and Fig. 5, where the backlash-induced spikes (50 Ω and $+\infty\ \Omega$) are so serious that they can be clearly identified in other cases. Fortunately, the backlash-induced spikes for the 2.5-15 Ω experiments were buffered by the damping force, such that the effective energy-harvesting bands were broader than that of the 50 Ω experiment. On the other hand, one may notice that the harvested power increases first and then decreases with the increase of the resistor value. This can be explained by the impedance matching theory[19]. According to the impedance matching theory, the best energy transfer capability can be achieved when the load resistance is equal to the internal resistance of the power source.

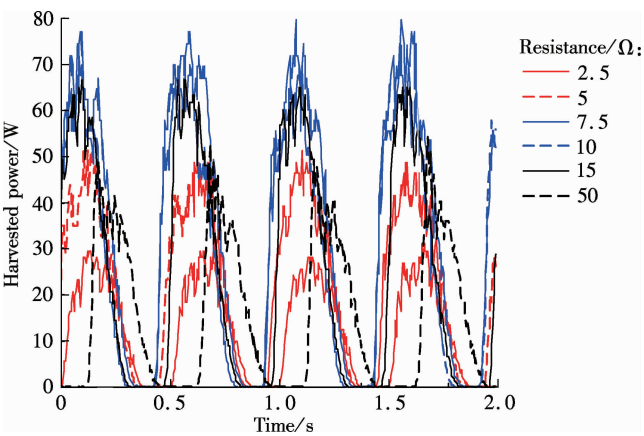

Fig. 6 Harvested electricity power in response to different load resistances

The energy harvesting efficiency η can be calculated as

$$\eta = \sum_{t=t_a}^{t_b} \frac{V_d^2(t)/R_d}{P_{in}(t)} \tag{16}$$

where $[t_a, t_b]$ denotes the time interval of interest for the efficiency calculation. To be meaningful, the range $[t_a, t_b]$ should be at least no shorter than one period of the vibratory excitation. Fig. 7 shows the change in the energy harvesting efficiencies. When tuning the resistance from 2.5 to 7.5 Ω, the efficiency increases with the rise of the load resistance. However, the efficiency drops if we further increase the resistance above 7.5 Ω, and the efficiency declines much faster when the resistance is higher than 15 Ω (about twice the internal resistance). As shown in Fig. 7, the maximum efficiency (27.49%) occurs at 7.5 Ω, which is almost identical to the internal resistance of the generator. This again proves the effectiveness of the impedance matching theory[19]. It also suggests that the impedance matching is a feasible method towards optimal energy harvesting with the maximum harvesting efficiency.

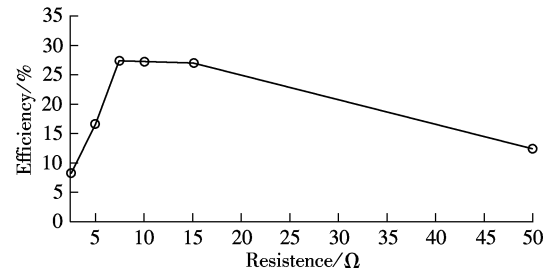

Fig. 7 Energy harvesting efficiencies with different load resistances

To calculate the variable damping resulting from the adjustable resistance, the following equation is used to calculate the equivalent damping coefficient c of the damper:

$$c = \sum_{t=t_a}^{t_b} \frac{F(t)}{\dot{x}(t)} \tag{17}$$

According to Fig. 4, one can plot the variable damping coefficient caused by the adjustable resistance. Fig. 8 shows the equivalent damping coefficients in response to different load resistances. In Fig. 8, No. 1 to No. 7 resistances denote 2.5, 5, 7.5, 10, 15, 50, and $+\infty\ \Omega$ (open circuit).

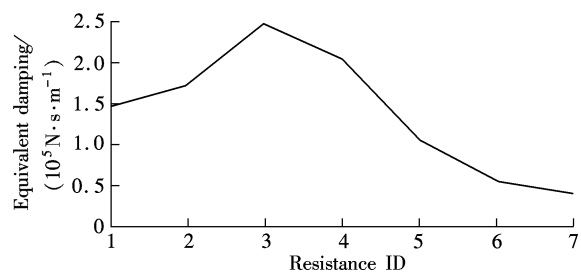

Fig. 8 Change in damping coefficients in response to different loads

Comparing Fig. 8 with Fig. 7, it is evident that the higher the energy harvesting efficiency, the greater the equivalent damping coefficient will be. The highest harvesting efficiency 27.49% occurs at 7.5 Ω load, which leads to the greatest equivalent damping coefficient 2.488×10^5 N·s/m. The smaller efficiency 0% corresponds to $+\infty$ Ω load (open circuit), where 3.987×10^4 N·s/m is the smallest equivalent damping coefficient among all the seven experiments. Based on the experimental results, one can conclude that, through adjusting the load resistance of the electromagnetic energy harvesting, one can obtain variable damping forces for the damper using the structure as shown in Fig. 1.

4 Conclusion

In this paper, a variable hydraulic damper resulting from adjustable vibration energy harvesting is described. The variable damping force is achieved by changing the load resistor of the harvester. To facilitate energy harvesting, the bidirectional vibration acting on the two terminals of the damper was transformed into unidirectional rotation by the four check values. This unidirectional rotation was subsequently employed to drive a power generator to harvest the vibration energy. The present approach is validated by both theoretical analysis and experimental evaluation. An electromechanical model was developed to analyze the behavior of the structure. A prototype was fabricated and tested. Our test results demonstrate that, when connected with different resistance loads, the prototype damper has different equivalent damping coefficients ranging from 3.987×10^4 to 2.488×10^5 N·s/m. The present research provides a novel approach in designing variable dampers for vibration applications.

References

[1] Ren W, Zhang J, Jin J. The virtual tuning of an automatic shock absorber[J]. *Journal of Mechanical Engineering Science*, 2009, **223**(11): 2655-2662.

[2] Polycarpou P C, Komodromos P, Polycarpou A C. A nonlinear impact model for simulating the use of rubber shock absorbers for mitigating the effects of structural pounding during earthquakes[J]. *Earthquake Engineering & Structural Dynamics*, 2013, **42**(1): 81-100.

[3] Koylu H, Cinar A. The influences of worn shock absorber on ABS braking performance on rough road[J]. *International Journal of Vehicle Design*, 2011, **57**(1): 84-101.

[4] Hu H S, Jiang X Z, Wang J, et al. Design, modeling, and controlling of a large-scale magnetorheological shock absorber under high impact load[J]. *Journal of Intelligent Material Systems and Structures*, 2012, **23**(6): 635-645.

[5] Roundy S, Wright P K, Rabaey J. A study of low level vibrations as a power source for wireless sensor nodes[J]. *Computer Communications*, 2003, **26**(11): 1131-1144.

[6] Fodor M G, Redfield R. The variable linear transmission for regenerative damping in vehicle suspension control[J]. *Vehicle System Dynamics*, 1993, **22**(1): 1-20.

[7] Chen C, Liao W H. A self-sensing magnetorheological damper with power generation[J]. *Smart Materials & Structures*, 2012, **21**(2): 025014.

[8] Choi K M, Jung H J, Lee H J, et al. Feasibility study of an MR damper-based smart passive control system employing an electromagnetic induction device[J]. *Smart Materials & Structures*, 2007, **16**(6): 2323-2329.

[9] Sapiński B. Vibration power generator for a linear MR damper[J]. *Smart Materials & Structures*, 2010, **19**(10): 105012.

[10] Suda Y, Nakadai S, Nakano K. Hybrid suspension system with skyhook control and energy regeneration[J]. *Vehicle System Dynamics*, 1998, **28**(Sl): 619-634.

[11] Choi Y T, Wereley N M. Self-powered magnetorheological dampers[J]. *Journal of Vibration and Acoustics*, 2009, **131**(4): 044501.

[12] Choi S B, Seong M S, Kim K. Vibration control of an electrorheological fluid-based suspension system with an energy regenerative mechanism[J]. *Journal of Automobile Engineering*, 2009, **223**(4): 459-469.

[13] Aly A M, Zasso A, Resta F. On the dynamics of a very slender building under winds: response reduction using MR dampers with lever mechanism[J]. *Structural Design of Tall and Special Buildings*, 2011, **20**(5): 539-551.

[14] Fang Z, Guo X, Xu L, et al. Experimental study of damping and energy regeneration characteristics of a hydraulic electromagnetic shock absorber[J]. *Advances in Mechanical Engineering*, 2013, **2013**: 943528.

[15] Li C, Liang M, Wang Y X, et al. Vibration suppression using two-terminal flywheel. Part Ⅰ: modeling and characterization[J]. *Journal of Vibration and Control*, 2012, **18**(8): 1096-1105.

[16] Li C, Zhu R, Liang M, et al. Integration of shock absorption and energy harvesting using a hydraulic rectifier[J]. *Journal of Sound and Vibration*, 2014, **333**(17): 3904-3916.

[17] Li C, Liang M. Characterization and modeling of a novel electro-hydraulic variable two-terminal mass device[J]. *Smart Materials & Structures*, 2012, **21**(2): 025004.

[18] Papageorgiou C, Houghton N E, Smith M C. Experimental testing and analysis of inerter devices[J]. *ASME Journal of Dynamic Systems, Measurement, and Control*, 2009, **131**(1): 011001.

[19] Beh T C, Kato M, Imura T, et al. Automated impedance matching system for robust wireless power transfer via magnetic resonance coupling[J]. *IEEE Transactions on Industrial Electronics*, 2013, **60**(9): 3689-3698.

基于电磁能量回收和可调负载的可变阻尼作用

李 川[1] 朱荣荣[1] 冯 鑫[1] 杨 帅[2]

([1] 重庆工商大学装备系统服役健康保障重庆市级国际联合研究中心,重庆 400067)
([2]Department of Mechanical Engineering, University of Ottawa, Ottawa K1N 6N5, Canada)

摘要:采用可调的振动能量回收方法,提出了一种面向半主动振动系统应用的新型变阻尼装置. 该阻尼装置利用油液在液压缸中的流动来驱动电磁发电机,从而回收振动能量,同时液压缸的两端产生阻尼作用. 采用可调的电阻负载来改变振动能量的回收能力,进而实现了阻尼作用的可变调节. 理论分析和实验评估验证了所提出的可变阻尼调节系统的有效性,在系统与不同电阻负载相连接的条件下,阻尼系统原理样机的等效阻尼系数可以实现在 $3.987\times10^4\sim2.488\times10^5$ N·s/m 之间变化. 结果表明,该系统通过负载调节振动能量回收能力,实现了阻尼装置的阻尼作用可变调节.

关键词:可变阻尼器;振动;能量回收;电磁发电机;负载
中图分类号:TH703.62